Modelling the Relative Humidity Inside Flat Plate Collectors

Stephan Fischer, Fabian Marquez

University of Stuttgart, Institute for Building Energetics, Thermotechnology and Energy Storage (IGTE)[1], Pfaffenwaldring 6, 70550 Stuttgart, Germany

Abstract

A mathematical model based on physical phenomena is introduced to model the relative humidity within flat plate collectors. Using the model, the water vapor which enters and leaves the collector as well as the water which is ad- and desorbed by the thermal insulation material during operation can be calculated. The paper describes the model and shows its application on three different collectors exposed Kochi, India. The water masses which enter and leave the collector during one month of operation as well as the water masses which are adsorbed and desorbed by the thermal insulation material for the three flat plate collectors are presented. This knowledge can be used for the design of an accelerated aging test procedure for flat plate collectors. The results are discussed and an outlook for future work is given.

Keywords: relative humidity in flat plate collectors, adsorption isotherm, water vapor adsorption, thermal insulation material, air volume flow through collectors, accelerated aging test, lifetime prediction

1. Introduction

During their lifetime solar thermal collectors are exposed to a variety of partially overlapping aging effects. These are introduced on the one hand from the system type and the mode of operation resulting in different inlet temperatures of the heat transfer fluid. On the other hand site-specific climatic conditions have an important impact on the aging process as shown by B. Traub et al. (2012) and P. Kofler et al. (2013).

To assess and judge the durability and reliability of solar thermal collectors for different system types and different locations a test procedure which takes into account these different ageing processes is needed which goes far beyond the existing durability and reliability test sequences which are documented in the ISO 9806 (2013) testing standard. Within the German project *Speed*Coll "Development of Accelerated Ageing Tests for Solar Thermal Collectors and their Components" a test procedure was developed taking into account ageing processes a solar thermal related to UV radiation, salty environment, humidity temperature cycles and high temperatures. The test procedure is described by S. Fischer (2017).

Within the follow-up project *Speed*Coll2 "Estimation of the service life of solar collectors and its components" the developed test procedures will be reviewed and further developed. This paper will introduce a model of the relative humidity within flat plate collectors as a basis for the review of the humidity test developed in the *Speed*Coll project. To model the relative humidity within the collector 3 different mass transfer phenomena were taking into account:

1. Air exchange between the ambient and the inner of the collector
2. Diffusion of water vapor through the leaks of the collector
3. Adsorption and desorption of water vapor by the thermal insulation material

2. Collectors investigated

For the modelling of the relative humidity 3 different collectors were investigated. Within the Tab. 1 the main characteristics of the 3 collectors are summarised.

[1] On July 1, 2018 the Institute for Building Energetics (IGE), the Institute of Thermodynamics and Thermal Engineering (ITW) with its Research and Testing Centre for Thermal Solar Systems (TZS) as well as the Institute of Energy Storage (IES) have been merged to the Institute for Building Energetics, Thermotechnology and Energy Storage (IGTE)

doi:10.18086/eurosun2018.12.04 Available at http://proceedings.ises.org

Tab. 1: Characteristics of the collectors investigated

Characteristic	Collector 1	Collector 2	Collector 3
Thermal insulation	Mineral wool	Mineral wool	Melamine foam
Collector ventilation	In and out in the air gap between absorber and transparent cover	In and out in the air gap between absorber and transparent cover	Through the thermal insulation in and out in the air gap between absorber and transparent cover
Absorber coating	selective	selective	selective
Transparent cover	Solar glass uncoated	Solar glass uncoated	Solar glass with AR coating

3. Measurements

To develop a model for the relative humidity within a flat plate collector the temperature as well as the relative humidity within the collector must be known in addition to the ambient temperature and the relative humidity of the ambient air. All 6 *Speed*Coll test sites (Stuttgart (Germany), Freiburg (Germany), Zugspitze (Germany), Gran Canaria (Spain), Sede Boker (Israel) and Cochi (India)) are equipped with extensive measuring sensors to measure the ambient conditions. At the exposure sites in Stuttgart (Germany) and Kochi (India) additional sensors were installed to measure the temperature and relative humidity within the air gap between absorber and transparent cover of the three collectors listed in Tab. 1.

Fig. 1 shows the sensors installed in the air gap and outside the collector. In Fig. 2 two of the collectors with installed combined temperature and humidity sensors are shown together with the cooling unit installed in Kochi, India. The sensors are visible as bright dots in the middle of the two collectors shown.

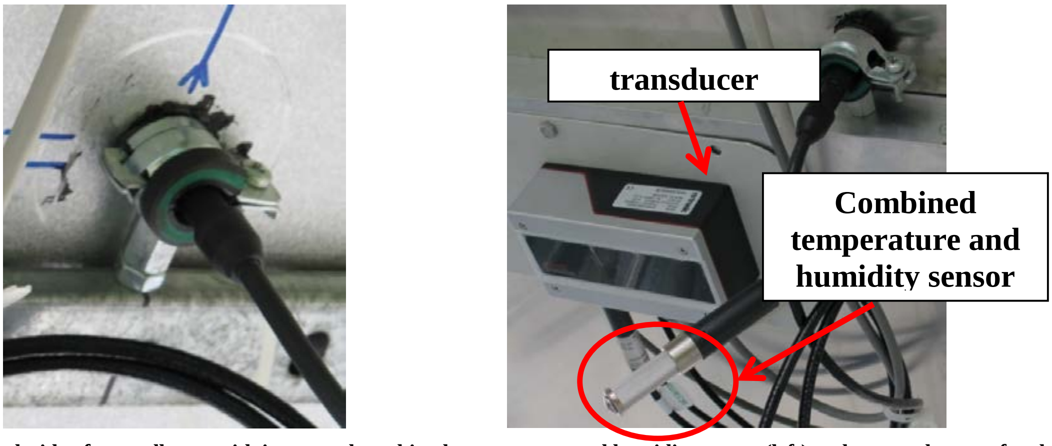

Fig. 1. Back side of one collector with immerged combined temperature and humidity sensor (left) and a second sensor for the measurement of the ambient temperature and relative humidity (right)

Fig. 2. Cooling unit (right) and collector 1 and collector 2 with combined temperature and humidity sensor (left) at the exposure site Kochi, India

In Fig. 3 measured data for three consecutive days (16.-12. – 18.12.2014) of the hemispherical irradiance, ambient temperature and the resulting temperature in the air gap between absorber and transparent cover of all three collectors are displayed. The maximum absorber temperature is kept by approx. 80 °C with the cooling unit. The difference in the air gap temperature of the three collectors is due to the different thermal performance. The corresponding relative humidity (rH) of the ambient and in the air gap of the three collectors can be seen in Fig. 4.

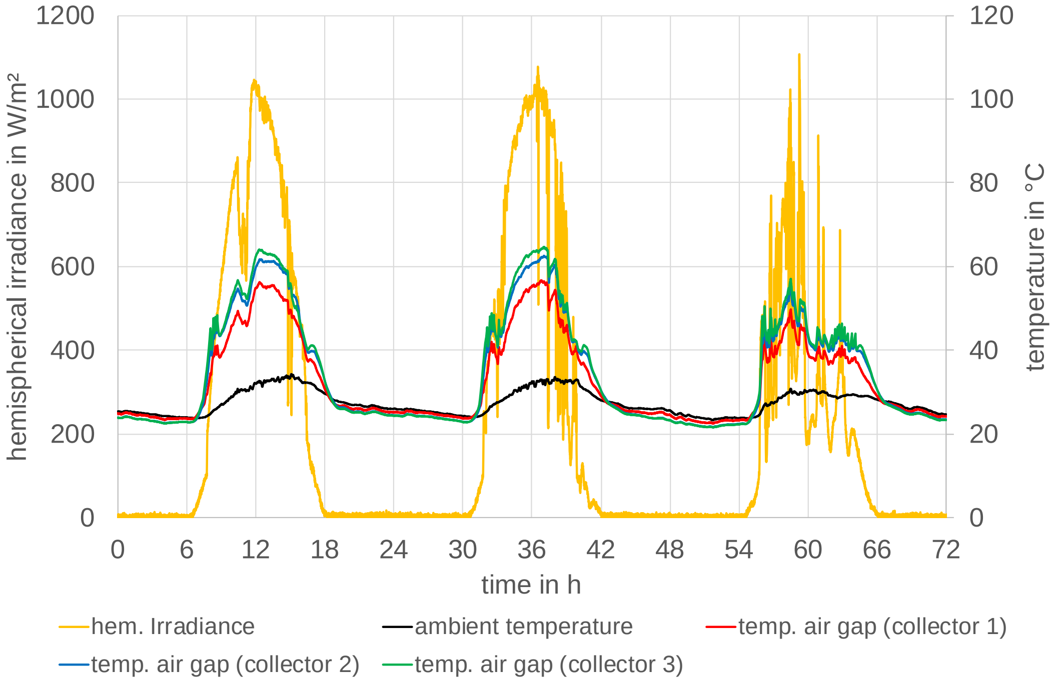

Fig. 3. Measurement for three consecutive days of the hemispherical irradiance, ambient temperature and the resulting temperature in the air gap between absorber and transparent cover of all three collectors at the exposure site Kochi, India

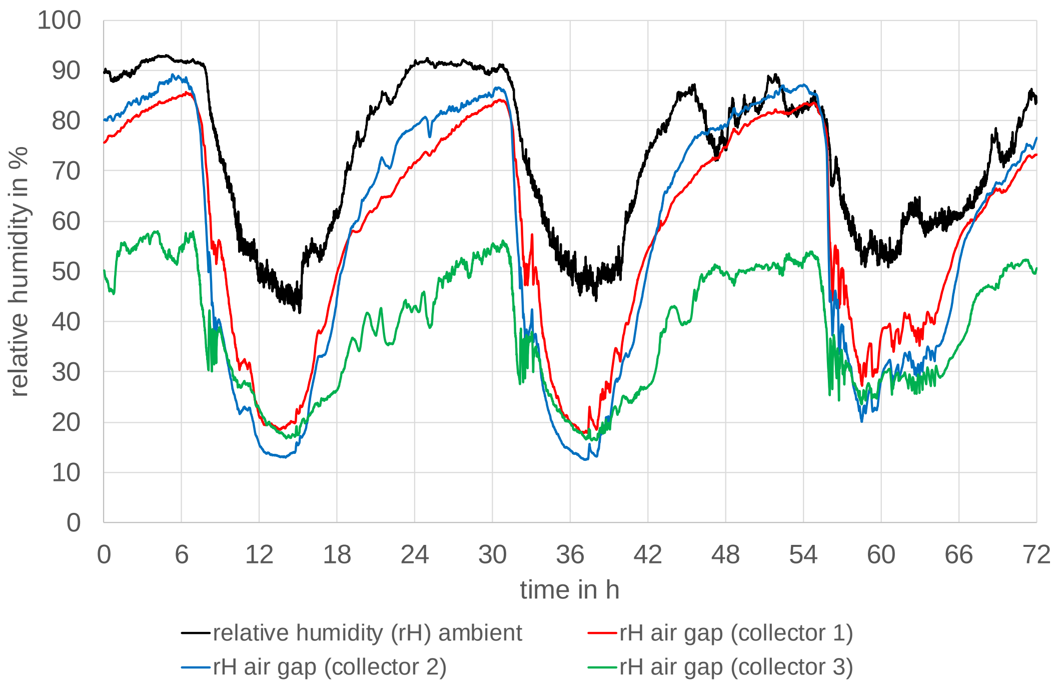

Fig. 4. Measurement for three consecutive days of the relative humidity of the ambient and in the air gap between absorber and transparent cover of all three collectors at the exposure site Kochi, India

The relative humidity of the ambient shows the expected development: high during night time (no irradiance, low ambient temperature) and low during daytime (irradiance, high ambient temperatures). The relative humidity within the air gap between absorber and transparent cover follows in principle the development of the relative humidity of the ambient. However, it is for all three collectors always lower and at times with high temperatures within the collector (high irradiance) significant lower. The relative humidity within collector 1 and 2 are very similar due to the use of the same collector ventilation strategy and similar thermal insulation material (mineral wool). Collector 3 shows a different behaviour due to the use of melamine foam and the ventilation though the side insulation.

The goal of the mathematical model described in the next section is to derive parameters which allow for the simulation of the relative humidity in the air gap between the absorber under any ambient conditions.

4. Mathematical model for the relative humidity

The model consists on a differential equation, which was derived from a mass balance of water vapor into the air gap between the absorber and the glass cover. For this, the ad- and desorption of water vapor by the insulation material, the diffusion of water vapor through the leaks of the collector and the transport of humidity caused by the air flowing through the ventilation openings of the collector were taken into account. The corresponding water mass flows were expressed as function of adjustment factors, which include all the unknown parameters for their direct calculation. The value of these were determined by using the least squared method based on measuring data recorded for three collectors in December 2014 in Kochi/India for a period of one month.

The adsorption behaviour is given by the so called adsorption isotherm curves. It represents the dependence of the mass fraction of water into the insulating material on the relative humidity of the surrounding air by a constant temperature. The IUPAC (International Union of Pure and Applied Chemistry) classifies the adsorption isotherms into six types depending on the shape of these curves (Sing et. al. (1985)). The type I describes the asymptotical saturation of the solid with condensed gas molecules. The types II and III are typical for materials which does not reach a saturation state during the adsorption process through unlimited multilayer condensation. The types IV and V describes the materials which reach a saturation state during a capillary condensation of gas molecules into the micropores (2 nm < $\emptyset_P$ < 50 nm) after a multilayer condensation into the macropores ($\emptyset_P$ > 50 nm), where the mass fraction of condensed gas into the material increased strongly with the relative humidity of the surrounding gas. The type VI is characteristic for materials which can undergo several capillary condensations before reaching the saturated state. The different behaviours are shown in Fig. 5

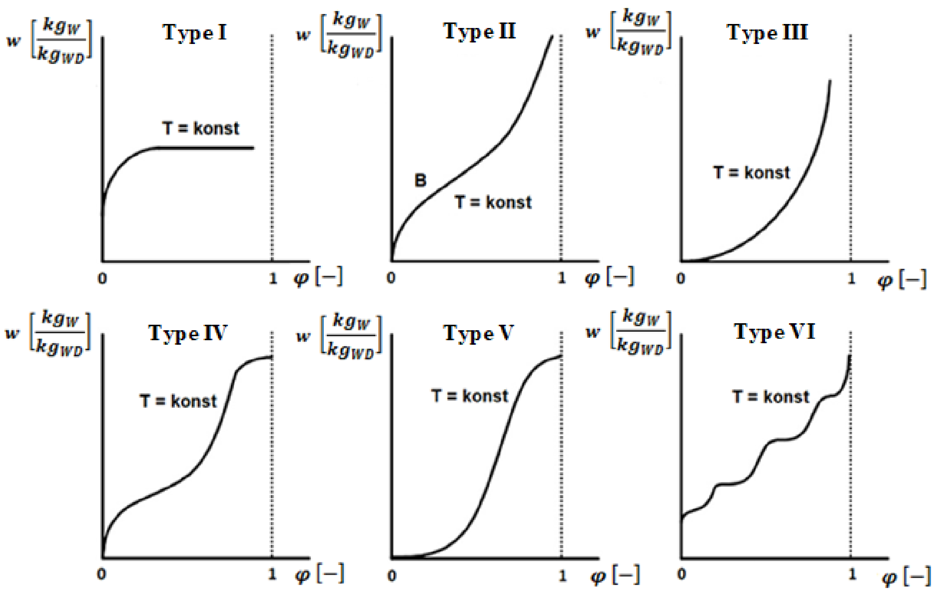

Fig. 5. IUPAC classification of adsorption isotherms

A linear behaviour of the adsorption isotherms was not included into this classification. It is described by the Henry's law Feng (2001). The temperature depending proportionality constant is given by the condensation enthalpy of adsorbed gas into the solid.

$$w_H(t) = k_H\big(T(t)\big) \cdot \varphi(t) \quad \text{(eq. 1)}$$

$$k_H(T(t)) = k_{H,o} \cdot \exp\left(\frac{k_{H,T}}{T(t)}\right) \quad \text{(eq. 2)}$$

$$k_{H,T} = \frac{\Delta H_H}{R_W} \quad \text{(eq. 3)}$$

As insulating materials in the collectors, mineral wool and melamine foam were used. Their adsorption behaviour can be well described with an adsorption isotherm of type IV and with the Henry's Law. Collet et al. (2011) proposed the GAB model (Guggenheim, Anderson and De Boer) for the adsorption isotherms of type IV as function of the adsorption enthalpy of the monolayer and the multilayer condensation, which was also used for the model development.

$$w_{GAB}(t) = w_{mG} \cdot C_G(t) \cdot k(t) \cdot \varphi(t) \cdot \left[\left(1 - k(t) \cdot \varphi(t)\right) \cdot \left(1 - k(t) \cdot \varphi(t) + C_G(t) \cdot k(t) \cdot \varphi(t)\right)\right]^{-1} \quad \text{(eq. 4)}$$

$$C_G(t) = \exp\left(\frac{E_a - E_m}{R_W \cdot T(t)}\right) \quad \text{(eq. 5)}$$

$$k(t) = \exp\left(\frac{E_L - E_m}{R_W \cdot T(t)}\right) \quad \text{(eq. 6)}$$

Since the adsorption enthalpies of water vapour into the insulating materials are unknown, they were expressed as function of adjustment factors, which are to be determined with the least squared method.

$$k_1 = \frac{E_a - E_m}{R_W} \quad \text{(eq. 7)}$$

$$k_2 = \frac{E_L - E_m}{R_W} \quad \text{(eq. 8)}$$

The mass flow of water vapour out or into the insulating material is given by the time derivate of the used equation for the adsorption isotherm curve.

$$\dot{m}_{ads} = m_{IM} \cdot \frac{d}{dt}\left(w(t)\right) \quad \text{(eq. 9)}$$

The diffusion mass flux through the leaks of the collector is proportional to the partial pressure difference of water vapour between the ambient air and the air in the air gap between absorber and transparent cover. The proportionality constant is given by the diffusion coefficient of water vapour into air, the gas constant for water, the average temperature between the ambient air and the mentioned space, the diffusion resistance factor and the flow distance of the vapour through the leaks.

$$\dot{m}_D''(t) = -\frac{D(t)}{R_W \cdot T_m(t) \cdot \mu \cdot \delta} \cdot \left(p_{d,c}(t) - p_{d,a}(t)\right) \quad \text{(eq. 10)}$$

$$D(t) = 0.231 \cdot 10^{-4} \cdot \frac{98100\ \text{Pa}}{p} \cdot \left(\frac{T_m(t)}{273\ \text{K}}\right)^{1,81} \quad \text{(eq. 11)}$$

$$\dot{m}_D(t) = k_D \cdot \frac{D}{R_W \cdot T_m(t)} \cdot \left(p_{d,c}(t) - p_{d,a}(t)\right) \quad \text{(eq. 12)}$$

$$k_D = \frac{A_D}{\delta \cdot \mu} \quad \text{(eq. 13)}$$

The area of the leaks, through which water diffusion can occur, the diffusion resistance factor and the flow distance of the vapour through the leaks are brought together into the constant k_{Diff}.

The volume flow of air through the ventilation openings is modelled with a power law as function of the driving pressure difference for the air buoyancy due to a temperature difference between the ambient air and the space between the glass cover and the absorber. The corresponding mass flow of air is then calculated with the specific volume and the water content of the humid air at the ambient conditions for each measurement.

$$\dot{V}_B(t) = k_p \cdot \Delta p_T(t)^n \quad \text{(eq. 14)}$$

$$\Delta p_T(t) = \rho_N \cdot T_N \cdot g \cdot h_c \cdot \left(\frac{1}{T_a(t)} - \frac{1}{T_c(t)}\right) \quad \text{(eq. 15)}$$

$$v_a(t) = \frac{(1 + 1{,}61 \cdot x_a(t))}{(1 + x_a(t))} \cdot \frac{T_a(t) \cdot R_a}{p} \quad \text{(eq. 16)}$$

$$\dot{m}_B(t) = \dot{V}_B(t) \cdot \frac{1}{v_a(t) \cdot (1 + x_a(t))} \quad \text{(eq. 17)}$$

The exponent n is assumed to be one. In consideration of the water vapour mass flow due to these mechanisms, the mass balance of humidity in the space between absorber and glass cover can be written as follows:

$$\frac{d}{dt}\left(m_{W,c}(t)\right) = -\dot{m}_{ads}(t) - \dot{m}_D(t) - \dot{m}_B(t) \cdot \left(x_c(t) - x_a(t)\right) \quad \text{(eq. 18)}$$

From this mass balance, a differential equation for the water mass fraction of the air in the space between absorber and glass cover was derived depending on the used adsorption model and the unknown variables for each mass flow.

Henry's Law:

$$\frac{d}{dt}(x_c(t)) = -c_{1,H} \cdot \frac{d}{dt}\big(w_H(t)\big) - c_2 \cdot \dot{m}_B{}^*(t) \cdot \big(x_c(t) - x_a(t)\big) - c_3 \cdot \dot{m}_D{}^*(t) \qquad \text{(eq. 19)}$$

$$c_{1,H} = \frac{m_{IM} \cdot k_{H,o}}{m_{a,c}} \qquad \text{(eq. 20)}$$

$$c_2 = \frac{k_p \cdot h_c}{m_{a,c}} \qquad \text{(eq. 21)}$$

$$c_3 = \frac{k_D}{m_{a,c}} \qquad \text{(eq. 22)}$$

$$\dot{m}_B{}^*(t) = \rho_N \cdot T_N \cdot g \cdot h_c \cdot \left(\frac{1}{T_a(t)} - \frac{1}{T_c(t)}\right) \cdot \big[v_a(t) \cdot \big(1 + x_a(t)\big)\big]^{-1} \qquad \text{(eq. 23)}$$

$$\dot{m}_D{}^*(t) = \frac{D}{R_W \cdot T_m(t)} \cdot \left(p_{d,c}(t) - p_{d,a}(t)\right) \qquad \text{(eq. 24)}$$

GAB-Model:

$$\frac{d}{dt}(x_c(t)) = -c_{1,GAB} \cdot \frac{d}{dt}\big(w_{GAB}(t)\big) - c_2 \cdot \dot{m}_B{}^*(t) \cdot \big(x_c(t) - x_a(t)\big) - c_3 \cdot \dot{m}_D{}^*(t) \qquad \text{(eq. 25)}$$

$$c_{1,GAB} = \frac{m_{IM}}{m_{a,c}} \qquad \text{(eq. 26)}$$

The parameters related with the mass balance ($c_{1,H}$, $c_{1,GAB}$, c_2, c_3) and the parameters related with the adsorption models (k_1, k_2, $k_{H,T}$) are set as adjustment variables and the water content of the air into the air gap between the absorber and transparent cover , which is calculated from the available measurement data, is set as target variable for the least squared method. For the calculation of the optimal set of parameters the Matlab® function "*lsqcurvefit*" was used. The relative humidity of this space is then derived from the corresponding value of temperature and the derived value for the water content for the air space. The time behavior of each mass flow is finally calculated with the optimal parameters from the least squared method and the mass of dry air to get the daily exchanged water quantities in the air space. For this, time integration for a time period of one day with the Matlab® function "*trapz*" is used.

$$m_{ads}(t) = m_{a,c} \cdot \int_0^t \dot{m}_{ads}(t)dt \qquad \text{If } \dot{m}_{Ads} > 0 \qquad \text{(eq. 27)}$$

$$m_{des}(t) = m_{a,c} \cdot \int_0^t |\dot{m}_{ads}(t)|\, dt \qquad \text{If } \dot{m}_{Ads} < 0 \qquad \text{(eq. 28)}$$

$$m_{in}(t) = m_{a,c} \cdot \int_0^t |\dot{m}_{trans}(t)|\, dt \qquad \text{If } \dot{m}_{tr}(t) < 0 \qquad \text{(eq. 29)}$$

$$m_{out}(t) = m_{a,c} \cdot \int_0^t \dot{m}_{trans}(t)\, dt \qquad \text{If } \dot{m}_{tr}(t) > 0 \qquad \text{(eq. 30)}$$

$$\dot{m}_{tr}(t) = \dot{m}_D(t) + \dot{m}_B(t) \cdot \big(x_c(t) - x_a(t)\big) \qquad \text{(eq. 31)}$$

5. Results

5.1. Comparison of measured and modelled relative humidity

Fig. 6, Fig. 7 and Fig. 8 show the comparison of the measured and modelled relative humidity in the air gap between absorber and transparent cover. For collector 1 and collector 2 the agreement between modelled (GAB Model) and measured values are very good. For collector 3 the agreement is not as good like for collector 1 and 2, however, the development of the relative humidity is still quite well modelled. The reason for the larger deviation is the fact that a significant portion of the humidity in the air entering the collector is absorbed locally in the insulation material which is passed by the entering air. This is not the case for collector 1 and collector 2 where the ambient air is entering directly the air gap between absorber and transparent cover without passing through the insulation material.

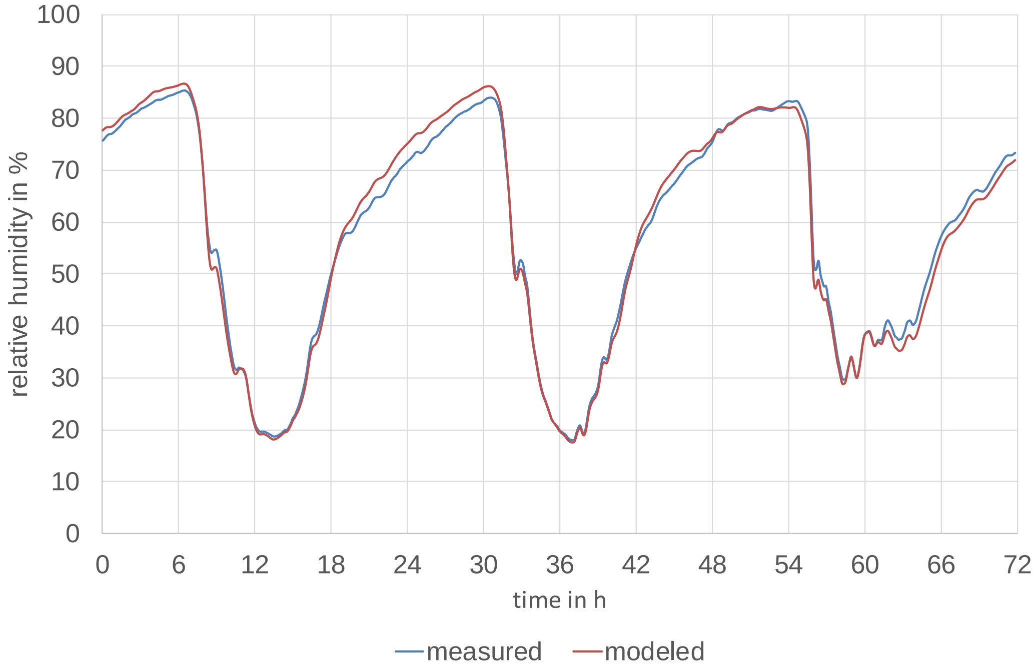

Fig. 6. Comparison measured and modelled relative humidity in the air gap between absorber and transparent cover of collector 1 at three consecutive days at at the exposure site Kochi, India

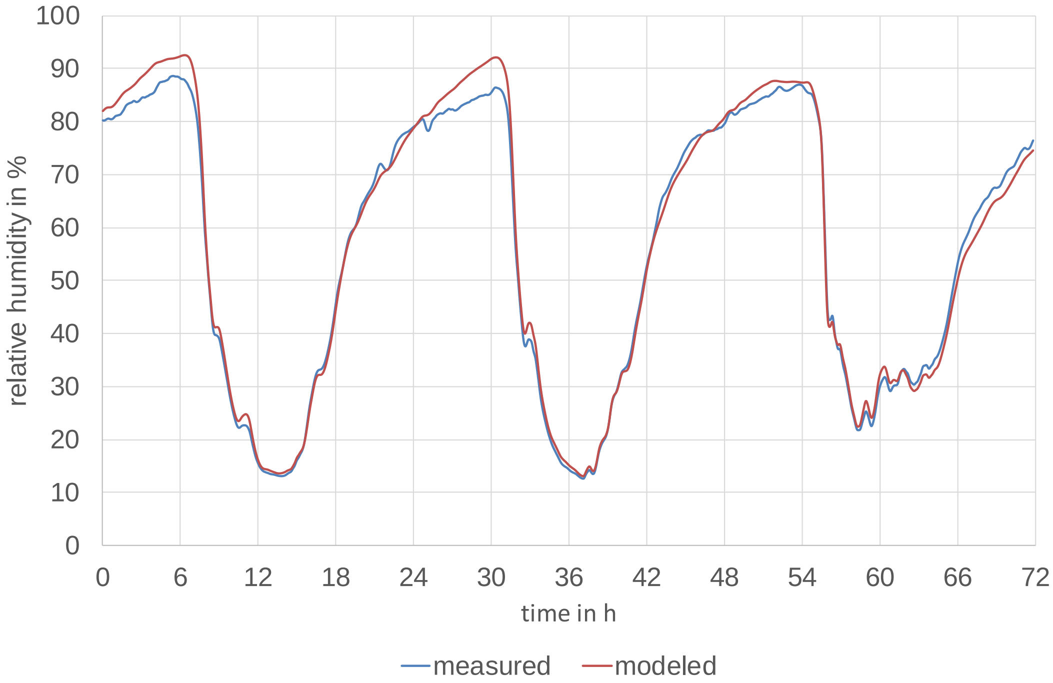

Fig. 7. Comparison measured and modelled relative humidity in the air gap between absorber and transparent cover of collector 2 at three consecutive days at at the exposure site Kochi, India

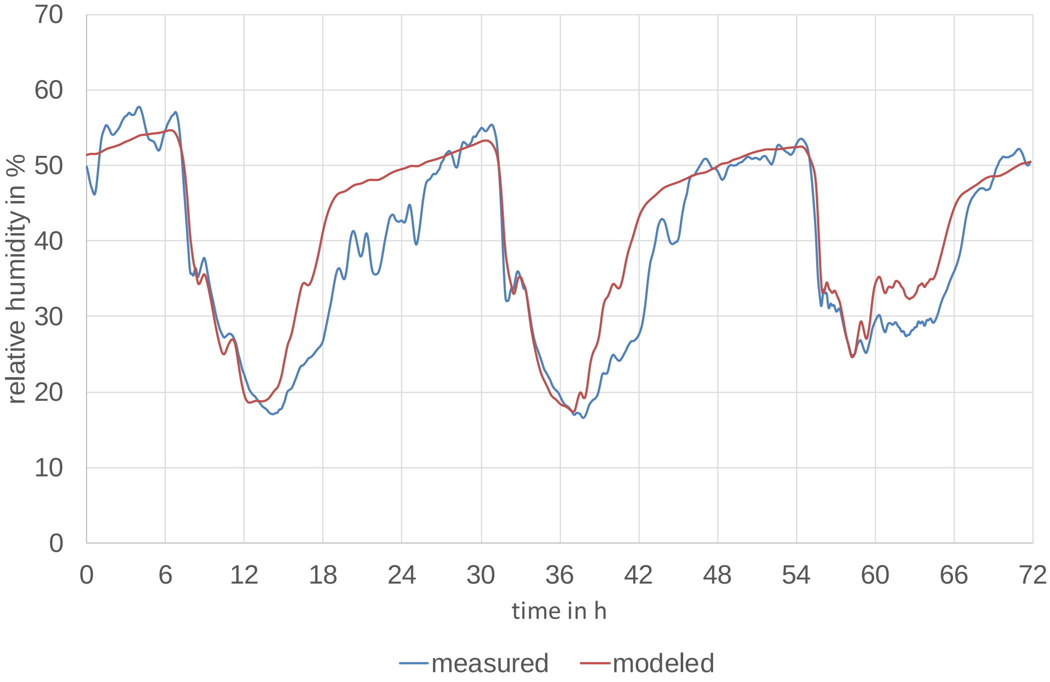

Fig. 8. Comparison measured and modelled relative humidity in the air gap between absorber and transparent cover of collector 3 at three consecutive days at at the exposure site Kochi, India

5.2. Water exchange between the inside of the collector and ambient

Using the equations shown in section 4 the water vapor adsorbed and desorbed from the insulation material can be calculated as well as the water vapor entering and leaving the air gap between the absorber and the transparent cover. Fig. 9 and Fig. 10 show the adsorbed (blue dots) and desorbed (red dots) water as well as the entering (green dots) and leaving (black dots) water for collector 2 and collector 3 for January 2015 at the exposure site Kochi, India. The solid lines represent the mean values for the month.

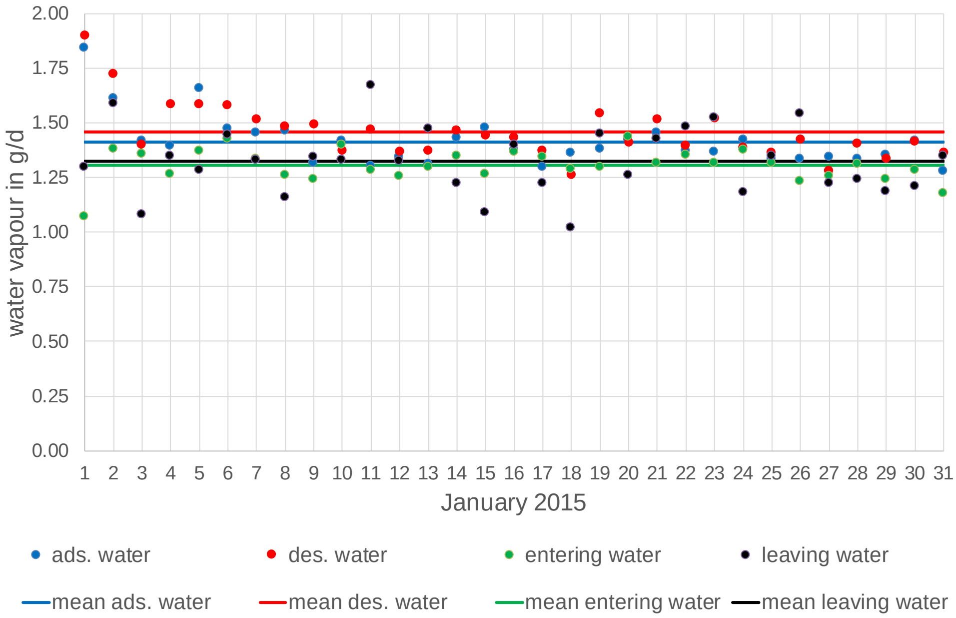

Fig. 9. Water vapour adsorbed (blue) and desorbed (red) by the insulation material and water vapour entering (green) and leaving (black) the air gap between the absorber and transparent cover for collector 2 at the exposure site Kochi, India

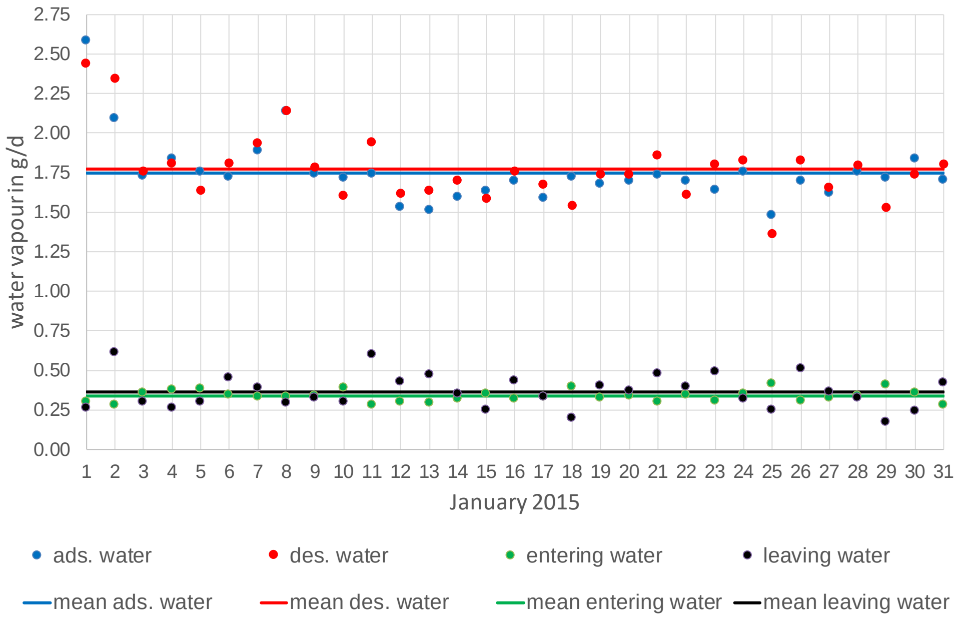

Fig. 10. Water vapour adsorbed (blue) and desorbed (red) by the insulation material and water vapour entering (green) and leaving (black) the air gap between the absorber and transparent cover for collector 3 at the exposure site Kochi, India

The amount of water adsorbed and desorbed as well as the water entering and leaving the air gap between absorber and transparent cover can be quite different from day to day depending on the weather conditions, however, the mean values show that in the long run the quantities (adsorbed/desorbed and entering/leaving) are the same.

A big difference in the amount of water entering and leaving the air gap between the absorber and the transparent cover can be observed for collector 2 and 3. This is due to the different ventilation strategies of the collectors. Collector 2 allows the ambient air to enter the air gap directly whereas the ambient air needs to pass through insulation material at collector 3 before entering the air gap and vice versa which results in ad- and desorption of water in the insulation material and a smaller air volume flow through the air gap, see Fig. 11 and thus to a smaller amount of water vapor entering and leaving the air gap between absorber and transparent cover, see Fig. 12.

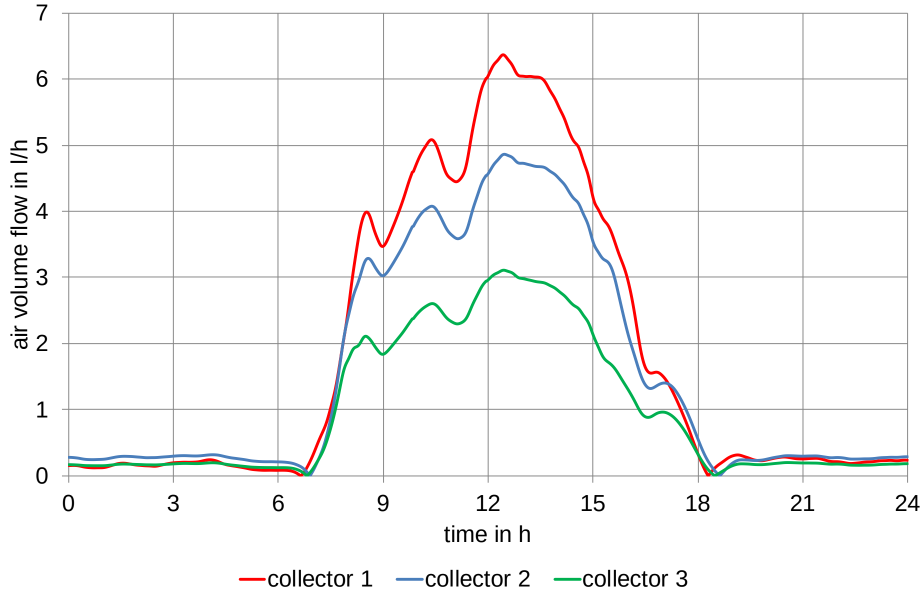

Fig. 11. Air volume flow through air gap between absorber and transparent cover on 16.12.2014 at the exposure site Kochi, India

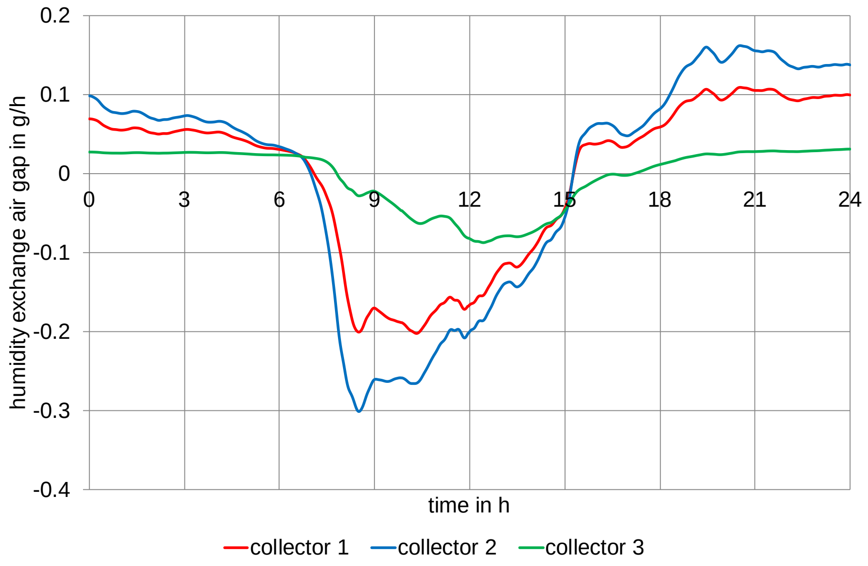

Fig. 12. Humidity exchange between ambient and air gap between absorber and transparent cover on 16.12.2014 at the exposure site Kochi, India

5.3. Interpretation of the results

Although the model is able to calculate the relative humidity in the air gap between the absorber and the transparent cover very well (see Fig. 6, Fig. 7 and Fig. 8) the values for the water vapor ad- and desorbed as well as the water vapor entering have to be questioned and discussed respectively.

In case of collector 1 and 2 which use mineral wool as thermal insulation material the amount of water vapor adsorbed and desorbed are in a realistic range when compared to indoor measurements of adsorption isotherms and mass increase when the material is charged with water vapor. However, for collector 3 using melamine foam as thermal insulation material there is a discrepancy between the calculated values and the theoretical values based on adsorption isotherms. Here the amount of adsorbed water vapor should be higher. The reason for this is the fact that on the one side most of the water vapor properly will locally adsorbed at the areas were the ambient air enters the collector through the insulation material and the air from the air gap leaves the collector through the insulation material. Whereas on the other hand only one sensor to measure the relative humidity is placed in the middle of the collector.

The volume flow of air entering and leaving the air gap between absorber and transparent cover is underestimated for all three collectors by the model. Realistic values should be 10 to 20 times higher. The reason for this is the overestimation of the diffusion of water vapor though leaks in the casing without air exchange and the placement of the temperature and humidity sensor at a location where the volume flow of air in the air is rather small compared to other locations. Nevertheless, the model is able to give a qualitative statement about the humidity balance within the solar collectors and their ventilation strategies.

6. Summary and outlook

A mathematical model based on physical phenomena is introduced to model the relative humidity within flat plate collectors. Using the model, the water vapor which enters and leaves the collector as well as the water which is ad- and desorbed by the thermal insulation material during operation can be estimated and conclusion can be drawn about the humidity balance in the investigated flat plate collectors and their ventilation system.

Based on this knowledge special indoor humidity test can be developed as part of an overall accelerated aging test procedure for flat plate collectors.

For further understanding and modelling of the humidity balance of flat plate collectors more detailed experiments using humidity and air flow sensors will be carried out within the SpeedColl2 project. These measurements are also used to validate CFD models which are also developed with in the project.

7. Nomenclature and Symbols

Tab. 2: List of symbols

Quantity	Symbol	Unit
Area	A	m^2
Diffusion coefficient of water in air	D	$m^2\ s^{-1}$
Constants of mass balance	c_1, c_2, c_3	-
Adsorption enthalpy of water (monolayer condensation)	E_a	$J\ kg^{-1}$
Mean adsorption enthalpy of water	E_m	$J\ kg^{-1}$
Adsorption enthalpy of water (multilayer condensation)	E_L	$J\ kg^{-1}$
Constants of GAB model	k_1, k_2	K
Constant for diffusion mass flux	k_D	m
Proportionality constant Henry's law	k_H	$kg\ kg^{-1}$
Constant for temperature dependence of Henry's law	$k_{H,o}$	$kg\ kg^{-1}$
Constant for temperature dependence of Henry's law	$k_{H,T}$	K
Flow coefficient of the ventilation openings	k_p	$m^3\ pa^{-1}\ s^{-1}$
Vertical distance between ventilation openings	h_c	m
Mass	m	kg
Mass flow	$\dot{m}$	$kg\ s^{-1}$
Mass flux	$\dot{m}''$	$kg\ m^{-2}\ s^{-1}$
Total pressure	p	Pa
Partial pressure of water	p_d	Pa
Gas constant	R_L	$J\ kg^{-1}\ K^{-1}$
Time	t	s
Temperature	T	K
Normed temperature	T_N	K
Mean temperature between collector and ambient	T_m	K
Specific volume of air	v	$m^3\ kg^{-1}$
Volume flow	$\dot{V}$	$m^3\ s^{-1}$
Water content of insulating material	w	$kg\ kg^{-1}$
Water content of insulating material after monolayer condensation	w_{mG}	$kg\ kg^{-1}$
Water content of air	x	$kg\ kg^{-1}$

Tab. 3: List of Greek symbols

Quantity	Symbol	Unit
Relative humidity	φ	-
Diffusion resistance factor	μ	-
Flow distance of the vapour through the leaks	δ	m
Normed density	ρ_N	$kg\ m^{-3}$
Adsorption enthalpy of water	ΔH_H	$J\ kg^{-1}$
Pressure difference for air buoyance	Δp_T	Pa

Tab. 4: Subscripts

Quantity	Symbol
Air	a
Water adsorption	ads
Air buoyance	B
Space between glass cover and absorber	c
Water diffusion	D
Desorption	des
GAB model	GAB
Henry's law	H
Inlet	in
Insulating material	IM
Outlet	out
Transported	tr
Water	w

8. References

Collet F., Achchaq F., Djellab K., Marmoret L., Beji H. 2011, „Water vapor properties of two hemp wools manufactured with different treatments, "Construction and Building Materials, pp. 1079-1085, 15 July 2011.

Feng J. 2001, "Interaction and permeability of water with liquid crystalline thermoset," University of Florida, Florida, 2001

Fischer, S. 2017. Test Procedure for Accelerating Aging of Solar Thermal Collectors, ISES Solar World Congress & SHC Conference, Abu Dhabi, 29.10. – 02.11.2017, ISES conference Proceedings (2017)

Kofler, P., Traub, B., Fischer, S., Drück, H., 2013. Alterungseinflüsse auf Sonnenkollektoren in gemäßigten und tropischen Klimazonen, Tagungsband zum 23. Symposium Thermische Solaranlagen, Seiten 138-139 (Kurzfassung), Kloster Banz, Bad Staffelstein, 24. – 26.04.13, ISBN 978-3-943891-10-2

Sing K. S. W., Everett D. H., Haul R. A. W., Moscou L., Pierotti R. A., Rouquérol J., Siemieniewska T., "Reporting physisorption data for gas/solid systems with special reference to the determination of surface area and porosity, "Pure and Applied Chemistry, Vol. 57. No. 4, pp.603-219, 1985.

Traub, B., Kofler, P., Fischer, S., Drück, H., 2012. Beanspruchung von Sonnenkollektoren unter Berücksichtigung unterschiedlicher Klimazonen und Anwendungen, Tagungsband zum 22. Symposium Thermische Solaranlagen, Seiten 154-155 (Kurzfassung), Kloster Banz, Bad Staffelstein, 09.05. – 11.05.12, ISBN 978-3-941785-89-2

9. Acknowledgements

The research projects "Development of Accelerated Ageing Tests for Solar Thermal Collectors and their Components", acronym "*Speed*Coll", and "Estimation of the service life of solar collectors and its components", acronym "*Speed*Coll2", are funded by the German Federal Ministry for Economic Affairs and Energy by resolution of the German Parliament and managed by Project Management Jülich (PTJ) under grant numbers 0325969B and 0325865B. The author gratefully acknowledges this support and take the responsibility for the contents of this publication.